Model-Free, Robust sliding mode control strategy for biohydrogen production in CST Reactor

Sánchez-Nextle Brenda[1]; Rodríguez-Jarquín José P.[1*]; Landeta-Escamilla Ofelia[1]; Martínez-Sibaja Albino[1]; Posada-Gómez, Rubén[2]

[1] Tecnológico Nacional de México - Instituto Tecnológico de Orizaba, Veracruz, México C. P. 94320
[2] Tecnológico Nacional de México – CRODE Orizaba, Veracruz, México. C.P. 94301.
* Correspondence: jose.rj@orizaba.tecnm.mx

ABSTRACT
Objective: To design, tune, and comparatively evaluate four model-free sliding mode control (MF-SMC) strategies to robustly stabilize biohydrogen production in a simulated continuous stirred-tank reactor (CSTR).
Design/methodology/approach: Robust control and optimization techniques are used in this study.
Results: MF-SCM strategies can handle nonlinearities and disturbances.
Limitations on study/implications: The study was conducted in a simulated environment; findings require validation in a physical laboratory-scale bioreactor.
Findings/conclusions: The MF-SMC strategy, tuned via genetic algorithms, is a viable and robust tool for controlling biohydrogen production, effectively handling nonlinearities and disturbances.

Keywords: Sliding mode control, biohydrogen production, CSTR, genetic algorithm, robust control.

Citation: Sánchez-Nextle B., Rodríguez-Jarquín, J. P., Landeta-Escamilla, O., Martínez-Sibaja, A. & Posada-Gómez, R. (2025). Model-Free, Robust sliding mode control strategy for biohydrogen production in CST Reactor. *Agro Productividad*. https://doi.org/10.32854/yz901p44

Academic Editor: Jorge Cadena Iñiguez
Associate Editor: Dra. Lucero del Mar Ruiz Posadas
Guest Editor: Daniel Alejandro Cadena Zamudio

Received: July 14, 2025.
Accepted: November 21, 2025.
Published on-line: December 11, 2025.

Agro Productividad, 18(11). November. 2025. pp: 125-140.

INTRODUCTION

Current hydrogen production is mainly based on the reforming of fossil fuels, such as natural gas, accounting for 90% of global production (Tayarani and Ramji, 2022). However, these conventional methods pose serious environmental problems, generating approximately 10 tons of CO_2 for every ton of H_2 produced, which contributes significantly to greenhouse gas emissions (Elgowainy *et al.*, 2024; Mazzoli *et al.*, 2024).

To address this challenge, research is being conducted to improve biological hydrogen production processes so that it can become a more sustainable source of energy. Current research has focused on optimizing various operational variables to obtain higher yields, which is one of the main challenges when using biological routes (Sanghvi *et al.*, 2024). A clear example is the study conducted by Rezk *et al.* (2023), where three key operational parameters were optimized in a membrane bioreactor: gas inlet flow

rate, pH, and rotor speed. By integrating an ANFIS model and the "Honey Bagder" algorithm, the optimal values for these variables were determined, which improved production yield from 23.8 L to 25.52 L, achieving an increase of 7.22%. On the other hand, Karapinar *et al.* (2020) studied the effect of hydraulic retention time (HRT) on hydrogen production in a packed bed reactor, finding that HRT values that were too low drastically reduced the conversion of glucose to H_2, demonstrating the existence of a critical operating range for maximum production.

Recent studies have highlighted significant experimental progress toward scaling up biological hydrogen production systems and implementing automatic control strategies. Pilot-scale reactors have been successfully operated, providing valuable data for assessing the feasibility and sustainability analysis that serves as reference for commercial-scale implementation (Zhang *et al.*, 2024). In this context, advanced control algorithms have been experimentally validated in hydrogen production systems, including fuzzy and adaptive sliding mode controllers, which have demonstrated reliable performance in handling nonlinearities and operational uncertainties (Kuterbekov *et al.*, 2024, Koundi *et al.*, 2025). Moreover, recent experimental evidence confirms the stability and robustness of Sliding Mode Control applied to bioreactors, reinforcing its potential for real-scale biohydrogen production (Yu *et al.*, 2024). These findings collectively underscore the ongoing transition from theoretical models to practical, automated, and scalable biological hydrogen production systems (Lu *et al.*, 2020, Gomez-Aquino *et al.*, 2025). In addition to optimizing operating parameters, studies have been conducted on robust control to manage the complex dynamics inherent in these processes. Works such as that of Kuterbekov *et al.* (2024) propose the use of a fuzzy control system to increase reactor capacity, highlighting its superiority in addressing the nonlinear characteristics of the system and achieving exceptional tracking of desired values even under model uncertainties. Regarding the use of Sliding Mode Control (SMC) in bioprocesses, studies have been conducted to improve the overall robustness of the system. Lopéz-Peréz *et al.* (2022), for example, designed a nonlinear sliding mode controller for a bioreactor, demonstrating that its algorithm was robust to parametric and system disturbances without the need for complete knowledge of the reaction rates. This type of control is particularly valuable because of its inherent robustness, an essential quality for systems with high uncertainty such as bioprocesses. In this context, Model-Free Sliding Mode Control (MF-SMC) represents a promising development. However, there is a gap in the literature on the systematic and comparative evaluation of different MF-SMC variants under a wide range of disturbances. Therefore, the overall objective of this work is to propose, implement in simulation, and comparatively evaluate four MF-SMC control strategies to maintain stable and close-to-target hydrogen production in a CSTR reactor under different disturbances. The specific objectives are: 1) to determine the optimal operating point of the system through sensitivity analysis and numerical optimization; 2) to specify, implement, and adjust MF-SMC control variants with different switching laws and gain schemes; and 3) to evaluate the robustness of the controllers against a set of 29 realistic disturbance scenarios.

It is important to note that this study is conducted entirely in a simulation environment, using the mathematical model of Aceves-Lara *et al.* (2008) migrated to Python. While this

approach allows for systematic evaluation under controlled conditions, the findings require experimental validation in a physical laboratory-scale bioreactor to confirm robustness under real operating conditions.

MATERIALS AND METHODS

Since this research is based on a simulation environment, the materials consisted mainly of software resources and computational models.

- Simulation platform: Python 3.9. Standard libraries such as NumPy, Pandas, Matplotlib, and Seaborn were used.
- Process model: The mathematical model developed by Aceves-Lara *et al.* (2008) was used.
- Optimization tools: A Genetic Algorithm (GA) implemented in Python was used.

Process model and operating point

The study was based on the pseudo-stoichiometric dynamic mathematical model of anaerobic fermentation developed by Aceves-Lara *et al.* (2008), which describes hydrogen production in a CSTR reactor. This model, consisting of nine ordinary differential equations, was migrated from MATLAB/Simulink to Python for integration with optimization and simulation tools. The system's dynamics are concisely represented in the equation (1):

$$\frac{d}{dt}\begin{bmatrix} Glu \\ Ace \\ Pro \\ Bu \\ X \\ CO_2 \\ H_2 \end{bmatrix} = K \cdot r - D\begin{bmatrix} Glu - Glu_{in} \\ Ace \\ Pro \\ Bu \\ X \\ CO_2 \\ H_2 \end{bmatrix} - \begin{bmatrix} 0 \\ 0 \\ 0 \\ 0 \\ 0 \\ q_{CO_2,gas} \\ q_{H_2,gas} \end{bmatrix} \quad (1)$$

In this equation, the state vector represents the concentrations of key compounds (glucose, acetate, propionate, butyrate, biomass, and dissolved CO_2 and H_2). The right-hand side concisely models the three fundamental phenomena governing the process: the biological reaction kinetics ($K \cdot r$), the reactor's hydraulic dynamics due to inflow and outflow (D), and mass transfer of gaseous products from the liquid to the gas phase (q_{gas}). This formulation served as the basis for all simulations and controller designs in this study.

To ensure the accuracy of the migration, the outputs of the original MATLAB/Simulink model were quantitatively compared with the Python implementation under identical steady-state conditions (glucose 20 g/L, and dilution rate 1 d^{-1}). As shown in Table 1, the steady-state hydrogen production values demonstrate excellent equivalence, with a relative difference consistently below 0.1% across all comparison points. The minor discrepancies observed in the initial transient phase are attributable to differences in the numerical solvers' default tolerances and the smoother, interpolated

Table 1. Quantitative Comparison of Steady-State Hydrogen Production in MATLAB and Python Models.

Time (d)	H_2 production MATLAB (mol L^{-1})	H_2 production Python (mol L^{-1})	Relative difference (%)
20	0.3102	0.3101	0.03
40	0.3102	0.3101	0.03
60	0.3102	0.3101	0.03
80	0.3102	0.3101	0.03
100	0.3102	0.3101	0.03

representation of inputs in Python, as opposed to the step changes in Simulink. This quantitative validation confirms the high fidelity of the migrated model for its use in simulation and controller design.

To establish a reference operating point, an exploratory sensitivity analysis was first performed, varying the glucose concentration in the influent (10-20 g/L) and the feed flow rate (2-8 L/d). Through exploratory scanning and subsequent optimization with the L-BFGS-B algorithm, it was determined that the maximum hydrogen production point (0.9289 mol/L) is reached with a glucose concentration of 20 g/L and a flow rate of 4.06 L/d. This value was established as the setpoint for the control system.

Piecewise linearization approach

Because the model presents a nonlinear and indirect relationship between the control variable (flow rate) and the control objective (H_2 production), it was decided to approximate this relationship using piecewise linearization. The operating domain was divided into three zones with different behaviors, obtaining linear equations for each one, which provided an explicit relationship that was fundamental for the design of the controllers (see Figure 1).

The linear models by section obtained a coefficient of determination (R^2) greater than 0.99, validating the high fidelity of the approximation.

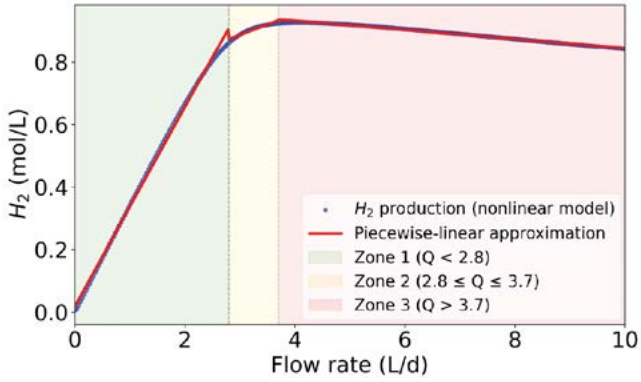

Figure 1. Piecewise linearized operating zones. Glucose fixed at 20 g/L.
Q denotes the flow rate. Linearization derived from the model equations.

Having established the operating point and linearization approach, the next step involves designing robust MF-SMC controllers that can effectively manage the nonlinear dynamics across all operational zones.

Controller design and tuning

Tracking error was defined as: $e(t) = \mathrm{H}_{2,setpoint} - \mathrm{H}_2(t)$. A first-order sliding surface is chosen as: $s(t) = e(t) + \lambda \int_0^t e(\tau)\, d\tau$, with $\lambda > 0$.

The four MF-SMC variants were implemented as shown in equations (2), (3), (4) and (5):

1. C1: Hyperbolic tangent function (tanh) with fixed gain.

$$Q = Q_{eq,i} + K_i \cdot tanh \frac{s}{\varepsilon} \tag{2}$$

2. C2: Hyperbolic tangent function (tanh) with adaptive gain.

$$Q = Q_{eq,i} + K_{adapt} \cdot tanh \frac{s}{\varepsilon} \tag{3}$$

3. C3: Saturation function (sat) with fixed gain.

$$Q = Q_{eq,i} + K_i \cdot sat \frac{s}{\varphi} \tag{4}$$

4. C4: Saturation function (sat) with adaptive gain.

$$Q = Q_{eq,i} + K_{adapt} \cdot tanh \frac{s}{\varphi} \tag{5}$$

Where: $Q_{eq,i}$ is the equivalent flow rate of the operational zone *i*. (obtained from the equations by piecewise linearization); K_i is the specific gain for each zone; K_{adapt} is the adaptive gain with predefined limits; ε, φ are the smoothness and bandwidth parameters for the *tanh* and *sat* functions.

The parameters of each controller were tuned using an GA and it was configured as follows:

- Population size: 100
- Number of generations: 100
- Selection method: Tournament selection (*tournsize*=3)
- Crossover method: Bland crossover (α=0.5), probability: 0.3

The fitness function combines tracking performance, control effort, and smoothness according to the following multi-objective cost (equation 3):

$$J = \int e(t)^2 \, dt + \omega_1 \int \left(Q(t) - Q_{eq}(t) \right)^2 + \omega_2 \int \left(dQ / dt \right)^2 \quad (3)$$

Where the weights (ω_1=0.1 and ω_2=0.1) are selected to balance accuracy, effort, and signal smoothness.

Robustness assessment and performance metrics

The robustness of the tuned controllers was evaluated in a total of 29 scenarios (17 individual and 12 combined) that simulate realistic and challenging process disturbances.

Various parameters of the model were modified, grouped into five categories:

Feeding

- P1: gradual breakdown of feeding glucose (0.2% daily)
- P2: ±20% variations in feed glucose concentration
- P3, P4: step disturbances and sinusoidal oscillations (±20%) in the feed flow.
- E1, E2: Glucose degradation (0.2% per day) with an initial concentration +20% and −20% above the optimum, respectively.

Kinetics

- P5, P6: Changes of ±10% and ±20% in maximum substrate uptake rates ($\mu 1, \mu 2$) to simulate variations in microbial activity.
- P7: Variation of ±20% in the half-saturation constant (K_1).
- P8, P9: Changes of ±20% in mass transfer coefficients $\left(K_{L\mathrm{H}_2}, K_{L\mathrm{CO}_2} \right)$.
- E3-E8: combinations of absorption rates ($\mu 1$, $\mu 2$), half-saturation constants (K_1), and oscillating inhibition to simulate favorable conditions up to scenarios of severe microbial stress.

Environmental

- P10, P11: Fluctuations in reactor temperature (±2 K) and ambient temperature (10-30 °C).
- P12, P13: Changes in atmospheric pressure (±0.04 bar) and vapor pressure (±10%).

Gaseous phase

- P14, P15: Simulated H_2 and CO_2 leaks from 0 to 10%.
- P16: Inhibitory effects on the reaction due to the accumulation of toxic by-products (±10 %).
- E9: Simultaneous H_2 and CO_2 leaks with oscillating inhibition of 5%.

Stochastic noise

- P17: Introduction of ±2% Gaussian noise in the simulated measurement of the H_2 sensor.

- E10, E11: Gaussian noise of ±2% in the H_2 sensor with descending and ascending ramp flow, respectively.
- E12: Gaussian noise of ±2% with step-like disturbances of +20% and −20%.

For noisy scenarios, 30 replicates were performed for each case-control combination to allow for rigorous statistical analysis. Performance was quantified using three key metrics: Steady-State Error (SSE), Maximum Amplitude, and Chattering.

These metrics were normalized using robust scales (median and interquartile range) to enable comparisons between scenarios and controllers within the deterministic analysis. It is important to clarify that, under this convention, more negative values in a metric indicate better relative performance (less error, less control effort), while positive values reflect suboptimal performance. This convention facilitates uniform interpretation across all evaluated contexts.

Justification of disturbance scenarios

The selection of the magnitude and form of disturbances is based on standardized control engineering practices and the inherently uncertain nature of the bioprocesses.

Stress-testing

The application of variations in key parameters is a standard practice un control engineering to quantify the robustness of a system (Bogaerts & Vande Wouwer, 2023). While there is no single universal standard establishing the thresholds of ±10% and ±20%, this ranges are reasonable and representative within the framework of sensitivity analysis and the variability inherent in bioprocesses, as it allows the system's response to be evaluated beyond small linear deviations and reveals sensitivities or instabilities that would not appear with smaller variations.

Variability of kinetic parameters

The kinetic parameters of a bioprocess model, such as maximum absorption rates ($\mu 1, \mu 2$) and half-saturation constants (K_1), are not fixed constants in a real system. Their variability is one of the main sources of uncertainty in bioprocess modeling and control (Abadli *et al.*, 2021; Hitzmann, 2020).

The causes of this variation may be due to microbial adaptation, substrate or product inhibition, or mixed cultures.

Stochastic noise simulation in H_2 sensor

Although ±2% may be considered a high noise level for a perfectly calibrated laboratory sensor, it is a relevant value for a stress test as it simulates the "worst case scenario" due to sensor aging, electromagnetic interference from nearby equipment (pumps, agitators), or biofilm formation on the probe. In addition, the stability of the control system is evaluated in the presence of "high noise levels" (Abadli *et al.*, 2021).

A robust controller must be able to filter these fluctuations without generating erratic or excessive control action (chattering), which is especially critical in sliding mode controllers.

Ramp, step, and sinusoidal disturbances

Step disturbances simulate abrupt and sustained events (*e.g.*, equipment failures or starts) to evaluate the controller's transient response, stability, and recovery speed. Ramp disturbances model slow, continuous shifts (*e.g.*, microbial activity degradation or out-of-calibration sensor) to test the system's ability to minimize tracking error in the face of gradual changes. Finally, sinusoidal signals represent periodic oscillations in the environment (*e.g.*, temperature fluctuations) to quantify the controller's ability to reject cyclic disturbances (Seborg *et al.*, 2017).

RESULTS AND DISCUSSION

Qualitative performance overview

To provide a qualitative overview of the controllers' dynamic performance, Figure 2 illustrates their temporal responses under two representative scenarios: one deterministic (P6) and one stochastic (E11).

In the deterministic scenario P6, which simulates a ±20% variation in substrate uptake rates, clear performance differences emerge. Controllers C2 and C3 exhibit nearly identical and highly effective responses, remaining consistently close to the setpoint. In contrast, controllers C1 and C4 show a transient deviation from this band before reconverging, highlighting distinct disturbance rejection capabilities.

Under the stochastic scenario E11, which includes ±2% Gaussian sensor noise and a ramp disturbance, all four controllers demonstrate robust performance. They successfully maintain hydrogen production largely within the optimal zone, with only minor, brief excursions. The presence of noise tends to obscure the finer performance distinctions observed in the deterministic case, resulting in more clustered behavior. This figure visually exemplifies the performance trade-offs that will be quantitatively analyzed in the subsequent sections.

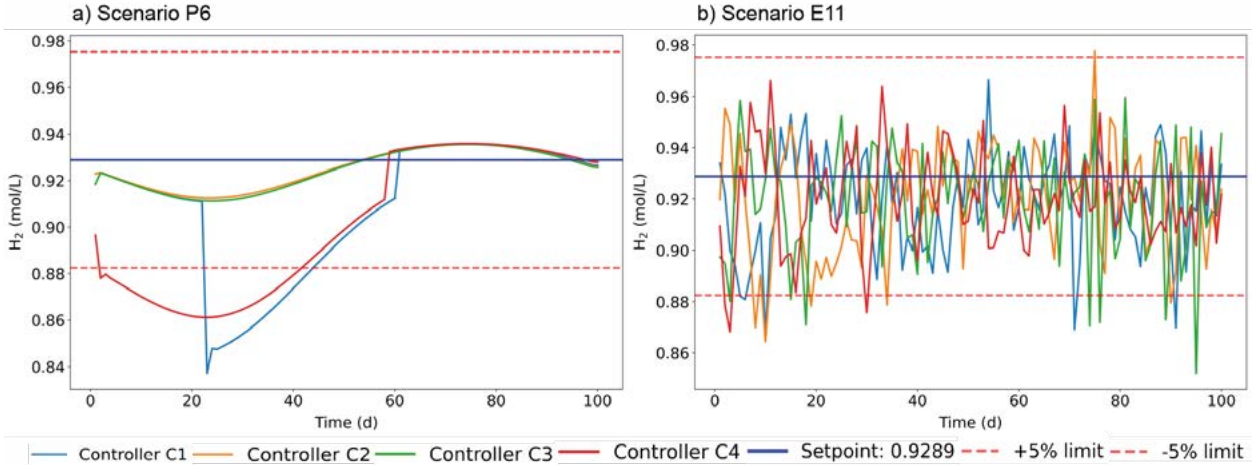

Figure 2. Dynamic response in representative scenarios. (a) deterministic and (b) stochastic scenarios. All data were obtained from numerical simulations of the proposed control strategies.

Robustness assessment in deterministic scenarios

Operational reliability and overall performance by category

A "successful case" was defined as one in which the controller managed to keep the SSE within 5% of the established setpoint. Table 2 summarizes the reliability of each controller, presenting the success rate in the overall analysis and broken down by category.

The results indicate that C3 is the most robust controller overall (68%), excelling in the Feed and Kinetics categories, which were the most challenging. On the other hand, perfect performance (100%) in the Environmental category and consistent performance in Leaks (75%) suggest an intrinsic robustness of the system to this type of disturbance, where the choice of controller is less decisive.

Similarity analysis for performance stratification

A visual inspection of the controllers' temporal responses revealed that their behavior was not heterogeneous among them, but rather that certain patterns were present. This prompted a similarity analysis, in which automatic classification was performed using statistical rules based on Manhattan distances on normalized performance metrics and subsequent validation with hierarchical clustering dendrograms, identifying four main behavior patterns. Table 3 shows the results of the classification using dendrograms.

For the final classification, the labels obtained using this method were chosen, as the statistical rules left some cases unassigned and visual evaluation is subjective. It was decided to integrate the "pairs" category into "subgroups" to avoid excessive divisions and maintain sufficient information for analysis, in addition to the fact that C4 only appeared in one isolated pair.

Analysis of Differentiated Cases

Two scenarios: P4 (feeding category) and P16 (leakage category) were identified as "Differentiated" due to the notable divergence in controller performance. Because these cases involve only two scenarios and fall below the threshold for formal statistical inference, a descriptive analysis was conducted as the primary investigative approach. The Coefficient of Variation (CV) was calculated for each metric and controller combination to quantify the relative variability and consistency of performance. The descriptive findings from the CV analysis are summarized in Table 4, which presents the performance ranking derived from these findings. Controllers were ranked from best to worst for each metric and case

Table 2. Percentage of success per controller in the overall analysis and per disturbance category.

Category	C1(%)	C2(%)	C3(%)	C4(%)
Global	56.00	60.00	68.00	52.00
Feeding	33.33	50.00	66.67	33.33
Kinetics	45.45	45.45	54.55	36.36
Environmental	100	100	100	100
Leaks	75	75	75	75

Table 3. Classification percentages using dendrograms.

Similarity	Frequency	Percentage (%)
Clustered	4	16
Pairs	6	24
Subgroups	13	52
Differentiated	2	8
Total	25	100

Table 4. Ranking of controllers by case and metric (better → worse).

Case	SSE	Amplitude	Chattering
P4	C3>C2>C1>C4	C3>C2>C1>C4	C1>C3>C4>C2
P16	C3>C2>C1>C4	C3>C2>C1>C4	C4>C3>C1>C2

based on the CV-informed assessment of performance consistency and magnitude. It was found that:

- In both cases, C3 proved to be the most accurate (lowest ESS and Amplitude), while C4 was consistently the worst in these two metrics.
- Regarding chattering, a reversal was observed: C1 was the most effective in P4, while for P16, C4 was the best for smoothing the control signal.
- Case P16 showed extreme variability in chattering, with a CV of 94.16%, indicating severe instability in the control signal among some controllers when faced with this disturbance.

These cases demonstrate that, under certain critical conditions, the selection of the optimal controller depends on a trade-off between accuracy and control signal quality.

Analysis of clustered cases

The four controllers classified as "Clustered" (E4, E5, E7, E8) belong to the Kinetic category. In these scenarios, an almost perfect convergence of the four controllers was confirmed. The Intraclass Correlation Coefficient (ICC) was 1.0 for all metrics in all cases, indicating a total absence of variability. Manhattan distances were also close to zero.

Statistical Analysis of Feeding and Kinetics

Once the special cases had been isolated, the general behavior in the different categories was analyzed.

For these categories, the performance of group C1-C2-C3 was compared with controller C4. To do this, a "representative" controller was selected for each case, defined as the one whose composite score (average of the three normalized metrics) was closest to the group mean. After verifying the assumptions of normality (Shapiro-Wilk) and homoscedasticity (Levene), the corresponding hypothesis tests were applied: t-test or Mann-Whitney U, as appropriate. The results are shown in Table 5.

Table 5. Results of statistical tests for comparison between the Representative controller and C4.

Category	Metric*	Test	p Value	Significant
Kinetics	SSE	Mann-Whitney	0.318	False
	Amplitude	Mann-Whitney	0.383	False
	Chattering	Mann-Whitney	0.902	False
Feeding	SSE	t-test	0.584	False
	Amplitude	t-test	0.558	False
	Chattering	Mann-Whitney	1.000	False

Note: *Normalized metric.

No statistically significant differences ($p>0.05$) were found between the Representative and C4 controllers for the three-performance metrics evaluated for both categories, suggesting that, although their success rates vary, the quality of their performance in stabilizing the system is quantitatively equivalent.

Descriptive Analysis of Leaks and Environmental

Due to the small sample size ($n<5$), a descriptive analysis was performed for these categories, the results of which are presented in Table 6.

This analysis confirms and clarifies the robustness of the system, revealing three consistent patterns:

1. High consistency: standard deviations are extremely low (in the range of 1E-03 to 1E-06) for all metrics, indicating that the behavior of the controllers are highly predictable and stable in the face of environmental disturbances and leaks.
2. Greater accuracy of the Representative group: on the standardized scale, more negative values indicate better performance (lower error); therefore, although both

Table 6. Descriptive analysis for the categories of Leaks and Feeding.

Category	Metric*	Group	Mean	Median	Deviation
Leaks	SSE	R	−2.82E-01	−2.86E-01	6.60E-03
		C4	−7.92E-03	−9.07E-05	1.38E-02
	Amplitude	R	−3.66E-01	−3.79E-01	2.28E-02
		C4	−7.33E-02	−9.71E-02	4.14E-02
	Chattering	R	−1.75E-01	−1.75E-01	1.34E-04
		C4	−1.85E-01	−1.85E-01	5.12E-04
Environmental	SSE	R	−2.86E-01	−2.86E-01	2.78E-04
		C4	−2.00E-04	−1.64E-04	2.50E-04
	Amplitude	R	−3.80E-01	−3.80E-01	2.85E-04
		C4	−9.73E-02	−9.73E-02	1.80E-04
	Chattering	R	−1.75E-01	−1.75E-01	5.45E-06
		C4	−1.85E-01	−1.85E-01	1.60E-05

Note: *Normalized metric.

groups are effective, the C1-C2-C3 group achieves a higher level of accuracy and stability than C4 in these scenarios (*e.g.*, −0.286 *vs.* −0.0000907).

3. Control effort: in terms of the chattering metric, the medians are practically identical (*e.g.*, −0.175 *vs.* −0.185), demonstrating that both groups exert a comparable control effort to manage these disturbances.

Robustness assessment in stochastic scenarios

Performance reliability versus noise

The consistency of each controller was evaluated using the CV, calculated from the 30 replicates per case-metric combination. Reliability was classified as high (CV≤15%), moderate (15%<CV≤25%), or low (CV>25%). Table 7 summarizes the percentage of measurements that fell into each reliability category for each controller.

This analysis yields the following conclusions:

- The C4 controller is the most reliable and consistent, with 75% of its metrics, indicating that its performance is the least affected by sensor noise.
- At the other end of the spectrum, C3 is the most sensitive to noise, with more than half of its results classified as low reliability. Its behavior is therefore the least predictable under stochastic conditions.
- Controllers C1 and C2 occupy an intermediate position, showing high reliability but high percentages of low or intermediate reliability, respectively.

Statistical comparison and global performance ranking

To rigorously compare controller performance under stochastic conditions, a comprehensive statistical analysis was conducted as the primary investigation tool. Assumptions of normality (Shapiro-Wilk) and homoscedasticity (Levene) were first verified for each metric and scenario. Based on these assumptions, parametric (ANOVA, Welch's ANOVA) or nonparametric (Kruskal-Wallis) tests were applied to compare metrics between controllers. The results of these global statistical tests are presented in Supplementary Table 8 and confirmed the existence of statistically significant differences in all cases analyzed (all p-values $<<0.05$).

Following the confirmation of global significance, post-hoc pairwise comparisons were performed to establish the magnitude and nature of the differences between individual controllers. These post-hoc analyses provided detailed insight into which controllers performed significantly better or worse in each metric and scenario.

Table 7. Reliability percentage per controller.

Controller	High (%)	Moderate (%)	Low (%)
C1	58.3	8.3	33.3
C2	66.7	25.0	8.3
C3	41.7	0	58.3
C4	75.0	16.7	8.3

Table 8. Statistical test results for stochastic scenarios.

Case	Metric	Test Applied	p-value
P17	SSE	Welch ANOVA	1.50E-65
	Amplitude	ANOVA	3.43E-67
	Chattering	Kruskal-Wallis	1.22E-15
E10	SSE	Kruskal-Wallis	3.45E -22
	Amplitude	Kruskal-Wallis	4.95E -21
	Chattering	Kruskal-Wallis	5.46E-18
E11	SSE	ANOVA	1.52E-71
	Amplitude	ANOVA	3.83E-25
	Chattering	Welch ANOVA	4.90E-27
E12	SSE	ANOVA	7.88E-63
	Amplitude	Kruskal-Wallis	2.23E-21
	Chattering	Welch ANOVA	1.86E-14

To present the complex results from these statistical analyses in a concise and accessible format, a performance ranking was synthesized from the outcomes of the post-hoc comparisons. This ranking, presented in Table 9, serves as a visual summary of the statistical findings, where controllers are ranked from 1 (best performance) to 4 (worst performance) for each metric. In cases where *post-hoc* tests revealed statistical equivalence between controllers, ranks were averaged.

The key results of the robustness analysis were:

- Accuracy (SSE): Controllers C1 and C3 showed the best accuracy, with very similar results between them.
- Stability (Amplitude): Controller C4 was consistently superior in containing oscillations and minimizing error amplitude. These results, together with a high level of reliability, suggest that its design is the most effective for maintaining system stability under noise.
- Control effort (Chattering): Controller C3 showed a much more aggressive control signal, while controllers C1, C2, and C4 maintained lower levels, making them more suitable for practical applications where the aim is to protect the actuators.

In summary, these results allow us to establish clear guidelines: if maximum precision is the priority, C1 or C3 are viable options (the high chattering of C3 must be taken into

Table 9. Average global ranking by metric (lower is better).

Controller	SSE	Amplitude	Chattering
C1	2.25	2.75	2.00
C2	2.88	3.00	2.00
C3	2.38	2.63	4.00
C4	2.50	1.63	2.00

consideration). If stability and oscillation suppression are the priority, C4 is the best option, while for a balance between good performance and low control effort, both C1 and C4 are excellent alternatives.

Comparative analysis of overall performance

To synthesize the findings from the individual disturbance scenarios and provide a holistic view of controller performance, a global comparison was conducted. Figure 3 presents this analysis using heatmaps, which display the average normalized performance of each controller across all deterministic (a) and stochastic (b) scenarios.

The performance metrics (SSE, Maximum Amplitude, and Chattering) were normalized using a robust scale based on the median and Interquartile Range (IQR). This allows for a fair comparison across different metrics and scenarios. Consequently, in the heatmaps, more negative values (warmer, brighter colors) represent superior performance, while positive values (cooler, darker colors) indicate a less optimal response. It is important to note that each panel was normalized independently to highlight the performance hierarchy within each context (deterministic *vs.* stochastic).

The simulation study evaluated four MF-SMC variants tuned with a GA under a comprehensive set of 29 deterministic and stochastic disturbances. These results confirm the working hypothesis that MF-SMC approaches tuned by GA can robustly handle nonlinearities and disturbances while revealing a systematic trade-off: C1/C3 prioritize accuracy (lower SSE) whereas C4 prioritizes stability (reduced amplitude and higher consistency under noise). The observed pattern is plausibly explained by controller gain and switching behavior: higher corrective gain reduces steady-state error but increases high-frequency switching (chattering), thereby raising actuator effort and sensitivity to noise. This interpretation aligns with prior experimental evidence that sliding-mode controllers provide strong disturbance rejection in bioreactors, although those studies also highlight the need to mitigate chattering for practical deployment. The practical implication is explicit: choose C1/C3 when minimizing steady-state error is imperative; choose C4 when

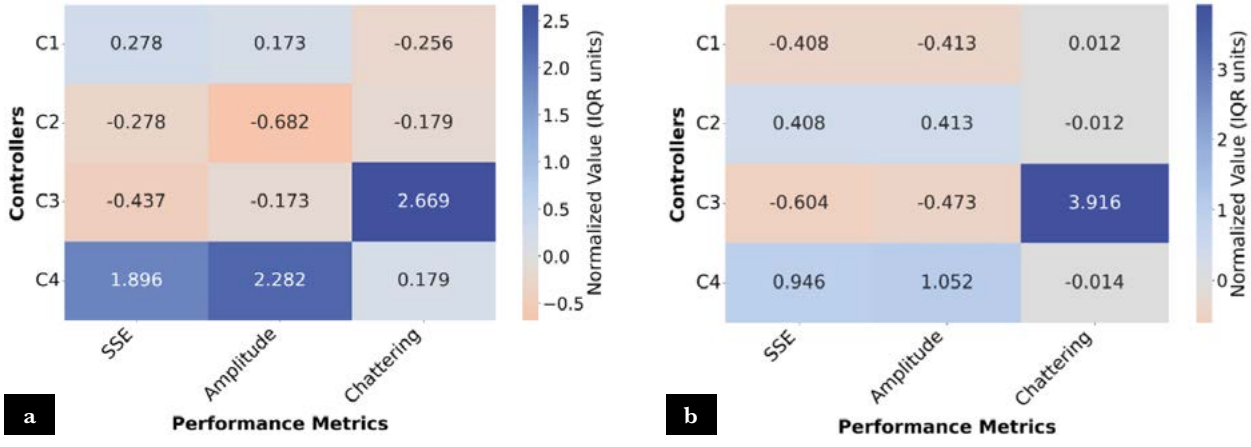

Figure 3. Global controller performance heatmap. (a) deterministic and (b) stochastic scenarios. Data were generated from simulation results and processed for visualization.

limiting oscillation amplitude and preserving actuator life under noisy measurements is the priority. The main limitation is that conclusions are derived from *in-silico* experiments on a migrated model; laboratory-scale validation is therefore required to confirm applicability and to identify unmodeled plant phenomena. As next steps we recommend experimental validation and a re-optimization of the GA objective to explicitly penalize chattering.

CONCLUSIONS

Four variants of model-free sliding mode control (MF-SMC) were designed and compared by simulation to regulate biohydrogen production in a CSTR; tuning was performed using a multi-objective Genetic Algorithm, and the evaluation included 29 disturbance scenarios.

Controllers C1 and C3 showed the best accuracy (lowest SSE), while C4 demonstrated the greatest ability to contain the amplitude of oscillations and the greatest consistency in the face of noise.

There is an operational trade-off between accuracy and control smoothness: improved accuracy is often accompanied by increased chattering, so controller selection should be based on operational priority (accuracy versus robustness and actuator protection).

The results should be considered as design recommendations derived from simulation analysis; experimental validation in a laboratory-scale bioreactor is necessary before practical implementation.

REFERENCES

Abadli, M., Dewasme, L., Tebbani, S., Dumur, D., & Vande Wouwer, A. (2021). An experimental assessment of robust control and estimation of acetate concentration in *Escherichia coli* BL21(De3) fed-batch cultures. *Biochemical Engineering Journal*, 174, 108103. https://doi.org/10.1016/j.bej.2021.108103

Bogaerts, P., & Vande Wouwer, A. (Eds.). (2023). Mathematical modeling and control of bioprocesses. MDPI. https://doi.org/10.3390/books978-3-0365-7141-6

Elgowainy, A., Vyawahare, P., Ng, C., Frank, E. D., Bafana, A., Burnham, A., Sun, P., Cai, H., Lee, U., Reddi, K., & Wang, M. (2024). Environmental life-cycle analysis of hydrogen technology pathways in the United States. *Frontiers in Energy Research*, 12. https://doi.org/10.3389/fenrg.2024.1473383

Gomez-Aquino, A., Vargas, A., & Moreno-Andrade, I. (2025). Biohydrogen production enhancement from organic solid waste using consecutive intermittent feeding strategies in a sequencing batch reactor. *Biomass Conversion and Biorefinery*. https://doi.org/10.1007/s13399-025-06539-z

Hitzmann, B. (2020). Bioprocess monitoring and control. MDPI. http://www.mdpi.com/books/pdfview/book/2827

Karapinar, I., Gokfiliz Yildiz, P., Pamuk, R. T., & Karaosmanoglu Gorgec, F. (2020). The effect of hydraulic retention time on thermophilic dark fermentative biohydrogen production in the continuously operated packed bed bioreactor. *International Journal of Hydrogen Energy, 45*(5), 3524-3531. https://doi.org/10.1016/j.ijhydene.2018.12.195

Koundi, M., El Fadil, H., Lassioui, A., & El Asri, Y. (2025). Adaptive sliding mode control of an interleaved buck converter–proton exchange membrane electrolyzer for a green hydrogen production system. *Processes, 13*(3), 795. https://doi.org/10.3390/pr13030795

Kuterbekov, K. A., Bekmyrza, K. Z., Kabyshev, A. M., Kubenova, M. M., & Shokatian-Beiragh, M. (2024). Fuzzy controller system utilization to increase the hydrogen production bioreactor capacity: Toward sustainability and low carbon technology. *International Journal of Low-Carbon Technologies*, 19, 667-675. https://doi.org/10.1093/ijlct/ctae026

Kuterbekov, K. A., Bekmyrza, K. Z., Kabyshev, A. M., Kubenova, M. M., & Shokatian-Beiragh, M. (2024). Fuzzy controller system utilization to increase the hydrogen production bioreactor capacity: Toward sustainability and low carbon technology. *International Journal of Low-Carbon Technologies*, 19, 667-675. https://doi.org/10.1093/ijlct/ctae026

Lopéz-Peréz, P. A., Rodriguez-Mata, A. E., Hernández-González, O., Amabilis-Sosa, L. E., Baray-Arana, R., & Leon-Borges, J. (2022). Design of a Robust sliding mode controller for bioreactor cultures in overflow metabolism via an interdisciplinary approach. *Open Chemistry, 20*(1), 120-129. https://doi.org/10.1515/chem-2021-0098

Lopéz-Peréz, P. A., Rodriguez-Mata, A. E., Hernández-González, O., Amabilis-Sosa, L. E., Baray-Arana, R., & Leon-Borges, J. (2022). Design of a Robust sliding mode controller for bioreactor cultures in overflow metabolism via an interdisciplinary approach. *Open Chemistry, 20*(1), 120-129. https://doi.org/10.1515/chem-2021-0098

Lu, C., Zhang, H., Zhang, Q., Chu, C., Tahir, N., Ge, X., Jing, Y., Hu, J., Li, Y., Zhang, Y., & Zhang, T. (2020). An automated control system for pilot-scale biohydrogen production: Design, operation and validation. *International Journal of Hydrogen Energy, 45*(6), 3795-3806. https://doi.org/10.1016/j.ijhydene.2019.04.288

Mazzoli, R., Pescarolo, S., Gilli, G., Gilardi, G., & Valetti, F. (2024). Hydrogen production pathways in Clostridia and their improvement by metabolic engineering. *Biotechnology Advances*, 73, 108379. https://doi.org/10.1016/j.biotechadv.2024.108379

Rezk, H., Olabi, A. G., Abdelkareem, M. A., Alami, A. H., & Sayed, E. T. (2023). Optimal parameter determination of membrane bioreactor to boost biohydrogen production-based integration of anfis modeling and honey badger algorithm. https://www.h2knowledgecentre.com/content/journal4908

Sanghvi, A. H., Manjoo, A., Rajput, P., Mahajan, N., Rajamohan, N., & Abrar, I. (2024). Advancements in biohydrogen production – a comprehensive review of technologies, lifecycle analysis, and future scope. *RSC Advances, 14*(49), 36868-36885. https://doi.org/10.1039/D4RA06214K

Seborg, D. E., Edgar, T. F., Mellichamp, D. A., & Doyle, F. J. (2017). Process dynamics and control (Fourth edition). Wiley.

Selişteanu, D., Petre, E., & Răsvan, V. B. (2007). Sliding mode and adaptive sliding2mode control of a class of nonlinear bioprocesses. *International Journal of Adaptive Control and Signal Processing, 21*(8-9), 795-822. https://doi.org/10.1002/acs.973

Tayarani, H., & Ramji, A. (2022). Life cycle assessment of hydrogen transportation pathways via pipelines and truck trailers: Implications as a low carbon fuel. *Sustainability, 14*(19), 12510. https://doi.org/10.3390/su141912510

Yu, Q., Wang, J., Huang, W., Li, X., Liu, Z., & Dong, H. (2024). Sliding mode integral separation pid control for hydrogen fuel cell systems. *Applied Sciences, 14*(17), 7650. https://doi.org/10.3390/app14177650

Zhang, Q., Jiao, Y., He, C., Ruan, R., Hu, J., Ren, J., Toniolo, S., Jiang, D., Lu, C., Li, Y., Man, Y., Zhang, H., Zhang, Z., Xia, C., Wang, Y., Jing, Y., Zhang, X., Lin, R., Li, G., … Tahir, N. (2024). Biological fermentation pilot-scale systems and evaluation for commercial viability towards sustainable biohydrogen production. *Nature Communications, 15*(1), 4539. https://doi.org/10.1038/s41467-024-48790-4

Zlateva, P. (2020). A modified sliding mode control of a nonlinear methane fermentation process. *E3S Web of Conferences*, 167, 05007. https://doi.org/10.1051/e3sconf/202016705007